euronoise 2021
25th to 27th of October
Madeira, Portugal - online

Design of a low-cost sound measurement device with wifi connectivity

Pedro Atanasio Moraga[1], Jaime Borrallo Rivera[2], Antonio Gordillo Guerrero[3,4], Juan Miguel Barrigón Morillas[1], David Montes González[1], Guillermo Rey Gozalo[1], Rosendo Vílchez-Gómez[1].

1Institute for Sustainable Regional Development (INTERRA), Lambda, Departamento de Física Aplicada, Universidad de Extremadura, Av. Universidad, s/n, 10003 Cáceres, Spain
2 Universidad de Extremadura, Av. Universidad, s/n, 10003 Cáceres, Spain
3 Departamento de Ingeniería Eléctrica, Electrónica y Automática. Universidad de Extremadura, Av. Universidad, s/n, 10003 Cáceres, Spain
4 Instituto de Computación Científica Avanzada de Extremadura (ICCAEx). Universidad de Extremadura, 06006 Badajoz, Spain.

Abstract
Environmental noise has become a major international concern as a polluting agent, affecting both health and wellness of the population. The use of low-cost sensors to assess people's noise exposure levels enables real-time monitoring of noise indicators at reasonable production costs.

An Arduino-based real-time sound measurement device is presented in this paper, with wireless download capability of the measured acoustic levels into a database. This device has been developed within the context of the low-cost sensor monitoring “SmartPolitech” project, a "living lab" of the School of Technology of the University of Extremadura in which technology contributes to energy efficiency and user comfort.

Keywords: Low-cost, Noise measurement, Noise Pollution, Wireless Acoustic Sensor Networks (WASNs)

1 Introduction

Incipient technological progress has allowed the development of new “low-cost” systems with high analysis capacity. These systems, many of them based on open source, enable the user to know a multitude of parameters in real time, such as activity, pulse and sound of the heart, air quality, temperature and sound in a bee-hive, etc [1-4]. Setting specific chips in a relatively simple way provides great versatility. Furthermore, these sensors are usually arranged in networks, mostly wireless, which enable monitoring of physical or environmental variables, turning the place where the sensors are installed into an experimental and cooperative space that provides a possibility of research into many aspects of everyday life. For example, through these networks it is possible to develop virtual replicas of communication infrastructures to help in their management [5], to track data about the mobility of people to model atmospheric pollution [6], to prevent floods through an early warning system [7], to know public flow inside buildings [8] or to identify relationships between physical, spatial and temporal parameters in urban environments [9,10]

Regarding acoustic, Wireless Acoustic Sensor Networks (WASNs) are becoming one of the most used tools to: measure: noise levels which people are exposed [11,12]; detect noise events; characterize the urban soundscape [13]; or predict psychoacoustic parameters with a certain accuracy [14]. These networks allow urban planners to carry out more effective measures regarding noise pollution.

In this paper, we present a sound measurement device based on open software (and hardware as much as possible) with wireless download capability. This device has been developed within the context of the low-cost sensor monitoring "SmartPolitech" project, inside the School of Technology of the University of Extremadura.

2 Methodology

The development of a low-cost sound measurement system, with capability to measure LAeq in real time, has been carried out following the guidelines of UNE-EN 61672-1:2014 standard [15] as far as electroacoustic specifications of the device are concerned: A-weighting, frequency range 16 Hz-16 kHz, Fast (F) integration and dynamic range of at least 60 dB at1 kHz.

The device was developed in four different phases (Figure 1):

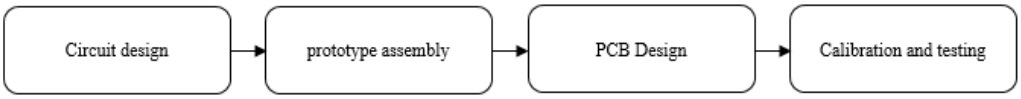

Figure1 – Device design process.

2.1.- Stage one. Circuit design

In the first stage, we designed the different electronic circuits that compose the low-cost sound measurement system. This stage was performed in two steps: First, hardware phase, in which the analogue audio signal processing was developed (Figure 2); Second, software phase, in which the audio signal was digitalized to be sent through the WEMOS Wi-Fi ESP8266 integrated device sensor.

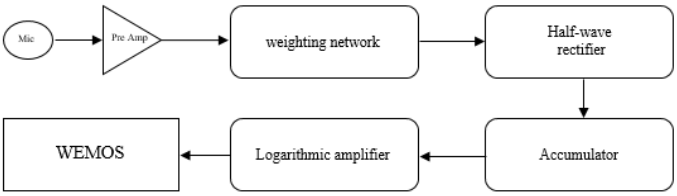

Figure 2 – Block diagram for the electronic circuit design.

Device specifications (Table 1) are decisive for choosing the elements that compose the electronic circuit that will be used to transform the analogue signals picked up by the microphone into digital via software.

Table 1 – Device characteristics.

Device characteristics	
A/D Converter Resolution	10 bits
Microphone sensitivity	17,78 mv/Pa
Communication protocol	IEE 802,11b
Frequency range	50Hz-16kHz
Memory	4Mb
Dynamic range	45dB-105dB
Evaluation parameters	LAeq
Weighting	A
Time filter	Fast

An electret 2 V-10 V omnidirectional condenser microphone, Panasonic model WM-61A, with a sensitivity of -35 dB ± 4 dB (0 dB = 1 V/Pa, 1 kHz), signal to noise ratio greater than 62 dB, has been chosen. This microphone has a nearly constant frequency response between 50 Hz and 15 kHz (Figure 3).

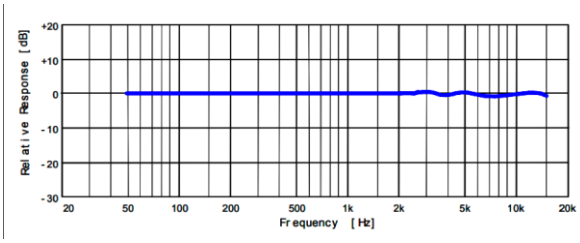

Figure 3 – WM-61A frequency response.

2.1.1.- Preamplifier design

To obtain the minimum required gain of the preamplifier, it is necessary to obtain its sensitivity, being the reference sensitivity 1 V/Pa.

$$S_{dB} = 20log\left(\frac{S(V/Pa)}{S_{ref}(V/Pa)}\right), \tag{1}$$

$$-35 = 20log\left(\frac{S(V/Pa)}{1(V/Pa)}\right); S = 0.01778\,V/Pa. \tag{2}$$

Minimum and maximum voltages provided by the microphone are calculated considering minimum and maximum sound pressure levels, 40 dB and 110 dB respectively, to be registered by the system:

$$Lp = 20log\left(\frac{P}{Pref}\right) \tag{3}$$

$$P = Pref\left(10^{\frac{Lp}{20}}\right), \tag{4}$$

$$V = S \cdot P, \tag{5}$$

Minimum and maximum voltages provided by the microphone will be 35 μV and 112.4 mV correspondingly.

The maximum voltage for the signal provided by the microphone is conditioned by the maximum voltage supplied by the power supply, 5 V. If 6.32 Pa (110 dB) is desired as the maximum pressure value picked up by the device, the maximum gain of the preamplifier will be:

$$G = \frac{V_S}{V_0} = \frac{5V}{112.4mV} = 44.5V. \quad (6)$$

For the preamplifier design, two linear amplifiers have been chosen in a row, with the TL071CP integrated from Texas Instruments. This has an operational amplifier in each integrated, one with a fixed gain of 20 kΩ and the other with a potentiometer of 50 kΩ. This way we can adjust the gain to the upper limit and avoid unwanted electrical noise at the same time.

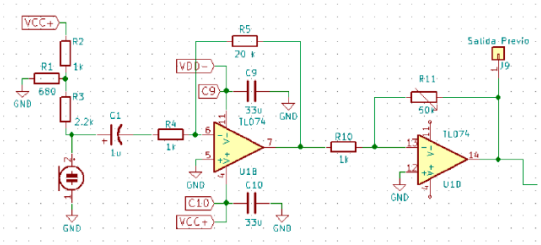

Figure 4– Preamplifier circuit made with Eeschema (Kicad).

2.1.2.- Weighting network design

A-weighting filter design has been carried out following the steps of Gantuz and Peacock´s project [16] and is based on the Argentinian standard IRAM 4074 [17], whose international equivalent is UNE-EN 61672-1:2014 [15]. In a theoretical way, this standard specifies that the A-weighting is realized with two poles in the complex frequency plane, located on the real axis at 20.6 Hz to provide the low frequency droop, and four poles on the real axis at frequencies 107.7 Hz, 737.9 Hz, and two poles at 12200 Hz to produce high frequency droop. The defined transfer function will be:

$$H_A(s) = \frac{4\pi^2 \cdot 12200^2 \cdot s^4}{(s+2\pi \cdot 20{,}6)^2 \cdot (s+2\pi \cdot 12200)^2 \cdot (s+2\pi \cdot 107{,}7) \cdot (s+2\pi \cdot 738)}. \quad (9)$$

The IRAM 4074 standard [17] specifies that the frequency A-compensation characteristics for this filter must be made with passive circuits of resistors and capacitors. The filter design is shown in the following figure (Figure 5).

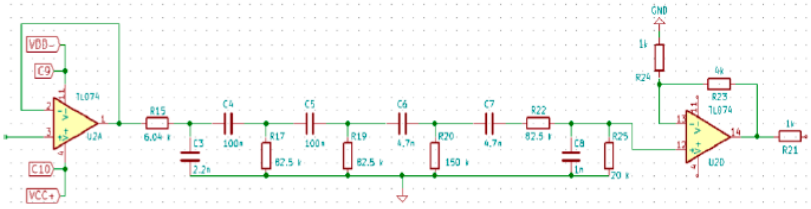

Figure 5 – A-weighting filter made with Eeschema (Kicad).

The negative feedback operational amplifier placed before the filter takes the high impedance signal picked up by the microphone and translates it to a very low impedance signal for the filter. In addition, to balance the voltage drop of the RC circuit, an amplifier has been placed at the output of the filter. The Texas Instruments TL074CN integrated has been used, which has four operational amplifiers on each integrated.

The frequency response of the filter is similar to the standardized A-weighting curve (Figure 6).

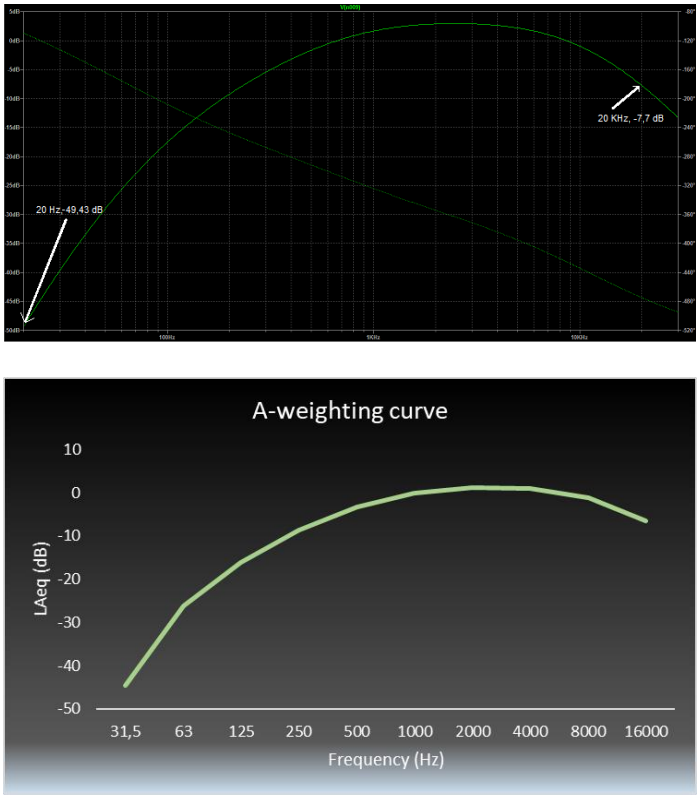

Figure 6 – A-weighting curve. Implemented filter and set curve.

2.1.3.- Half-wave rectifier and RC integrator circuit design

Next we developed a circuit to obtain the energy value of each sound wave picked up by the microphone. As the registered voltages are very small for very low-pressure levels, a precision half-wave rectifier and a RC circuit is needed to act as an integrator, providing a magnitude that is proportional to the sum of the energies of the different frequency components of the sound wave.

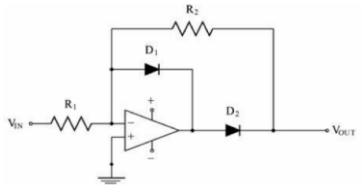

Figure 7 – Precision half-wave rectifier [18].

The use of diodes and resistors ensures that rectifier's operational amplifier does not exit the linear zone when the input signal changes his sign (positive or negative V_{in}). It works in a simple way:

- If V_{in} is positive, diode D_1 conducts and diode D_2 does not conduct, closing the feedback loop with D_1 and obtaining a zero voltage at the output, $V_{out} = 0\ V$.
- If V_{in} is negative, diode D_2 conducts and diode D_1 does not conduct, closing the feedback loop with D_2 and R_2, obtaining a voltage at the output $V_{out} = -V_{in} \cdot \left(\frac{R_2}{R_1}\right)$. If R_2 is equal to R_1, we get a perfect rectification.

This way, the operating frequency would now be limited by the diode capabilities and the properties of the operational amplifier in the linear region (gain-bandwidth-slow rate product).

For the temporal integration F (fast) of the signal, an RC circuit has been designed to provide its R.M.S. value. The multiplication of $R * C = 56700 * 2{,}210^{-6} = 0.12474s$ is equivalent to the time it takes for the capacitor to charge.

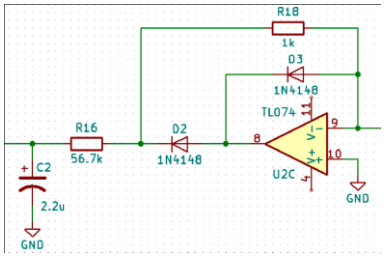

Figure 8 – Precision half-wave rectifier with RC filter made with Eeschema.

At first, the capacitor is discharged (Figure 9). As V_s grows towards positive values, the diode becomes forward polarized and the output voltage follow the input voltage. This procedure continues until time t_1, when the input decreases faster than the capacitor discharges through the load resistance. At this time, the output voltage follows the time evolution of this capacitor discharge. At instant t_2, the exponential drop of the output will intersect with the rise of the input voltage, time in which the diode will conduct again, continuing this process over time.

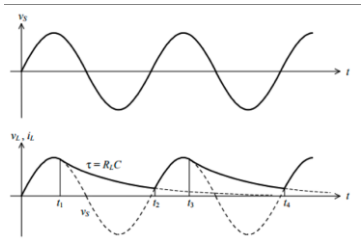

Figure 9 – In and out of the Precision half-wave rectifier with RC filter.

At the end of this stage, an amplifier has been inserted to compensate losses and adapt the signal to the next step.

2.1.4.- Logarithmic amplifier design

The circuit's converter has 10 bits of unipolar input range, from 0 V to 3.3 V, so 1024 voltage levels could be represented with a resolution of 0.00322 V per level. As the microphone registers a minimum voltage level of 35.5 µV (2 mPa), the device would have low resolution for low sound pressure levels. To solve this issue, it was decided to compress the signal proportionally to the logarithm of the input signal using a logarithmic amplifier, thus achieving a higher dynamic range.

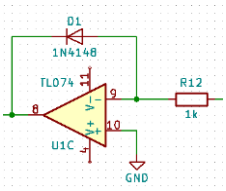

Figure 10 – Logarithmic amplifier for positive input made with Eeschema.

If we assume a negative input point on the operational, V_{-9}, and knowing that the input impedance to the amplifier is infinite, all the electric current is diverted to de diode D_1. Therefore, the diode will be direct polarized because we have a virtual ground at point V_{-9} of the amplifier (V_{-9} = 0 V).

$$\frac{V_{in}}{R_{12}} = I_s \cdot e^{\frac{V_{out}}{N \cdot V_T}} \rightarrow V_{out} = -N \cdot V_T \cdot ln\left(\frac{V_{in}}{R_{12} \cdot I_s}\right), \quad (10)$$

where:

- I_s is the reverse saturation current of the diode.
- V_T is the diode thermal voltage. This voltage is equal to k·T/q, where k is the Boltzmann constant $\left(k = 1.38 \cdot 10^{-23} \frac{J}{K}\right)$, q is the electron charge ($q = 1.609 \cdot 10^{-19} C$) and T is temperature in kelvins.

It can be seen that the output of the logarithmic amplifier is highly temperature dependent, in addition to being negative. To turn this signal positive, a linear amplifier has been placed. And a 10 kΩ potentiometer has been inserted to adjust the output signal. The Zener diode at the end of the analogue process limits the output to 3.3 V, protecting the WEMOS D1 Mini device.

Also, to calibrate the measured signal threshold, it has been necessary to set up a voltage divider connected to the positive pin of the amplifier (Figure 11).

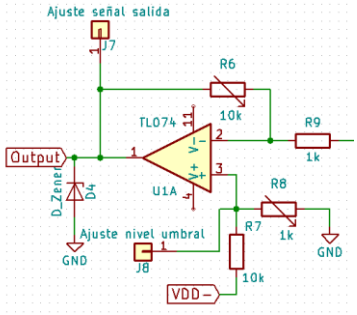

Figure 11 – Output amplifier and voltage divider for calibration of the threshold of the measured signal made with Eeschema.

2.1.5.- Circuit power supply

The device is powered by a 9 V battery, or a power supply, that provides a symmetrical voltage (+9V and -9V). A 7660S CPAZ has been used to adapt the power to +9V and -9V, at which the board operates. A LM7905C was used for the negative -5V output and a LM7805C has been used for the positive +5V output.

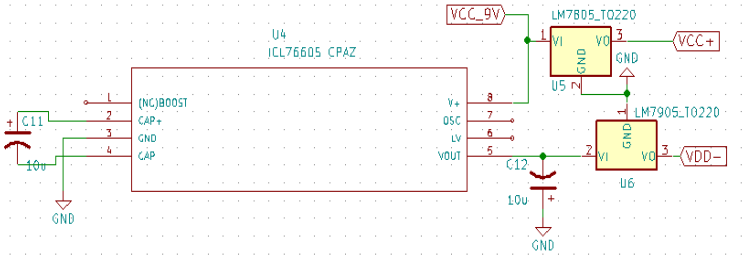

Figure 12 – Power supply circuit made with Eeschema.

2.2.- Stage 2. Printed Circuit Board (PCB) design and implementation.

Once all the circuits have been designed independently, it is time to put them all together to form the complete measurement device using Kicad's Eeschema software (Figure 13).

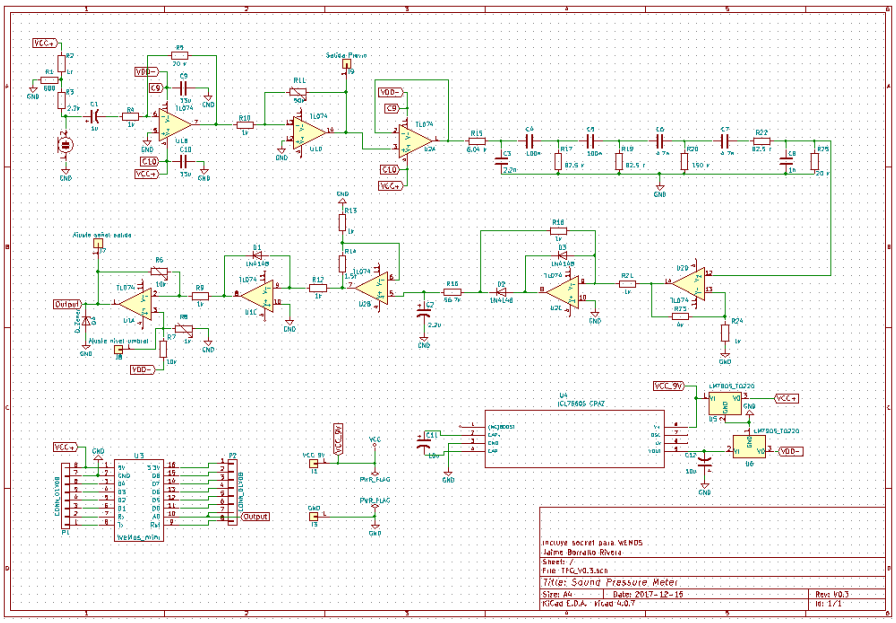

Figure 13 – Complete electronic circuit of the sound level meter made with Eeschema.

The design has been implemented with Pcbnew (Figure 14), including the socket for the Wemos D1 Mini device for wireless communication. This software makes it possible to send the complete board to production, avoiding the arduous job of wiring the individual circuits.

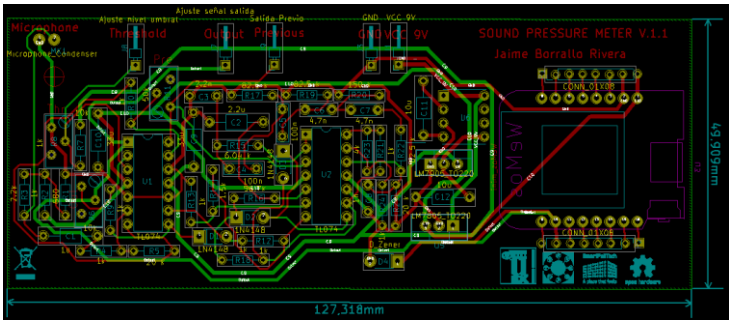

Figure 14 – Final electronic circuit of the sound level meter made with Pcbnew.

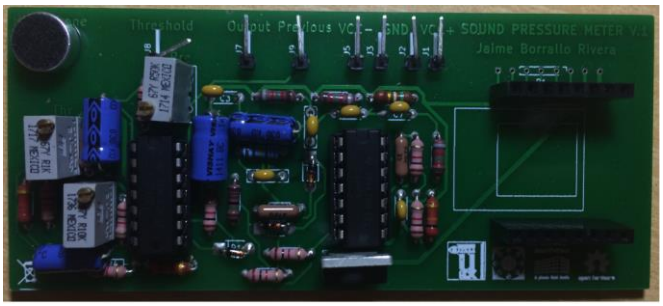

Figure 15 – Final electronic circuit of the sound level meter made with Pcbnew.

Due to initial design reasons, the power supply was added at a later time.

In a strictly aesthetic purpose, all the electronics circuits have been placed in a 3d design with two red and blue LEDs (Figure 16). Red led indicates that the power is on. Blue led indicates that the device is connected to the server: if it flashes once slowly, the device has successfully connected; if it flashes once faster, the device has successfully sent the sample.

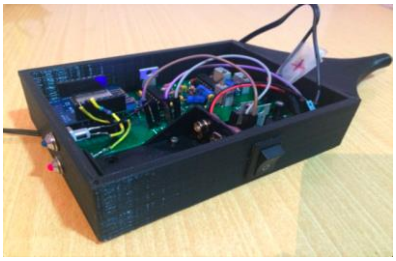

Figure 16 – Final design of the sound level meter.

2.3.- Stage 3. Device calibration

The device was calibrated according to ISO 1996-1 [19] and 1996-2 [20] standards, using a Brüel & Kjær 2250L class 1 sound level meter as reference, a Brüel & Kjær 4292L omnidirectional source, and a Brüel & Kjær 2713 amplifier.
First, A-weighted sound pressure level with fast integration of the B&K 2250L and voltage level of the device were taken, matching pressure to voltage. The sound pressure level was varied at a rate of 1 dB. This way, the potentiometers were set to adjust the input and output voltages to the values measured with the reference sound level meter.

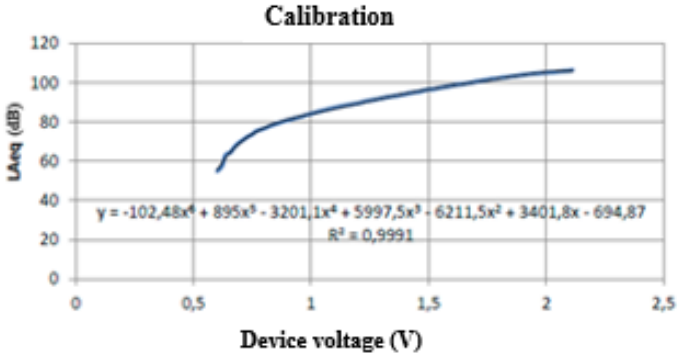

Figure 17 – A-weighted equivalent level vs. voltage approximation.

2.4.- Stage 4. Sending samples to server

Our device connects to the SmartPolitech network as a client of an MQTT client/server message server through the WEMOS D1 mini device. It is possible to change the time in which we want to send the measurements via Wi-Fi through a library that accepts the OTA (Over The Air) programming supported by the ESP8266 Wi-Fi chip included in WEMOS device.

3 Analysis and results

To analyse the reliability of the low-cost device, different measurements were performed, both with the reference sound level meter, describe before, and with our own device, exciting the environment with pink noise. The LAeq levels of both were recorded at 10 s intervals for 10 min, increasing the sound level gradually during this time.

Although with lower resolution, the device follows the time evolution of the reference sound level meter. In Figure 18 it can be seen that differences are greater at the lowest registered levels, decreasing as these levels increase. Overall, the levels measured help us to think that the device it can be useful to know the acoustic situation in several environments.

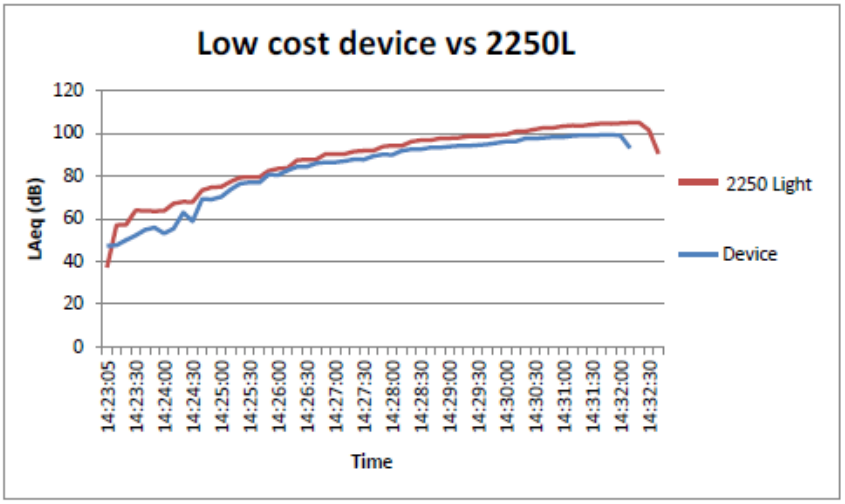

Figure 18 – Low-cost device vs Brüel&Kjær 2250L.

4 Conclusions

A low-cost device with the capability to measure A-weighted sound pressure levels has been designed. The different analogue circuits that compose it have been implemented and described. These circuits are responsible for conditioning the signal received in the microphone for subsequent digitalization, sending the collected levels to a server via Wi-Fi through the Wemos D1 Mini microcontroller. This device is suitable for wireless sensor networks.

Tolerances of low-cost components introduce some imprecision in the analogue circuit and can affect the received signals. In addition, the dependence on temperature of the logarithmic amplifier, the microphone sensibility (especially at low levels) and the system calibration are the main factors in the registered level differences. The device is designed to be as cheap as possible. Any improvements or upgrade to the analogue components will help to minimize the registered level differences and should not increase much the final price (for example, a much better microphone cost around 40€, instead of only 5€).

This project was developed both for an educational and research. The A-weighted equivalent level values registered are useful to get an idea of the acoustic situation of a place, but never to provide conclusive reports to the Administration. If annoying sound levels were measured with our device in a certain environment for a prolonged period of time, it would be time to carry out measurements with standardized sound level meters.

Acknowledgements

This project was co-financed by European Regional Development Fund (ERDF) and *Junta de Extremadura* (IB18050 and GR18107). This work was also supported by *Consejería de Economía, Ciencia y Agenda Digital* of *Junta de Extremadura*, European Union and European Social Fund (ESF) through grants for the strengthening of R&D&I through the mobility of postdoctoral researchers (PO17014) and by *Consejería de Economía, Ciencia y Agenda Digital* of *Junta de Extremadura* through grants for attracting and returning research talent to R&D&I centres belonging to the Extremadura Science, Technology and Innovation System (TA18019), where University of Extremadura was the beneficiary entity in both cases.

References

[1] Kumar S, Jasuja A. Air quality monitoring system based on IoT using Raspberry Pi. In: Proceeding - IEEE *International Conference on Computing, Communication and Automation, ICCCA 2017*. 2017. p. 1341-6.

[2] Prabha S, Raghav RS, Moulya C, Preethi KG, Sankaran KS. Analysis and Monitoring Air Quality System using Raspberry PI. In: *Proceedings of the 2020 IEEE International Conference on Communication and Signal Processing, ICCSP 2020*. 2020. p. 1385-9.

[3] Alvionita R, Ais RR, Wisana IDGH, Triwiyanto T, Setioningsih ED, Mak'Ruf MR, et al. Design of Cardiac Monitor for Multi Parameters. In: Proceedings - 2019 *International Seminar on Application for Technology of Information and Communication: Industry 40: Retrospect, Prospect, and Challenges, iSemantic 2019*. 2019. p. 423-8.

[4] Imoize AL, Odeyemi SD, Adebisi JA. Development of a low-cost wireless bee-hive temperature and sound monitoring system. *Indonesian Journal of Electrical Engineering and Informatics*. 2020;8(3):476-85.

[5] Steyn WJVDM, Broekman A. Development of a digital twin of a local road network: A case study. *Journal of Testing and Evaluation.* 2023;51(1).

[6] Lu Y. Beyond air pollution at home: Assessment of personal exposure to PM2.5 using activity-based travel demand model and low-cost air sensor network data. *Environmental Research*. 2021;201.

[7] Acosta-Coll M, Solano-Escorcia A, Ortega-Gonzalez L, Zamora-Musa R. Forecasting and communication key elements for low-cost fluvial flooding early warning system in urban areas. *International Journal of Electrical and Computer Engineering*. 2021;11(5):4143-56.

[8] Perra C, Kumar A, Losito M, Pirino P, Moradpour M, Gatto G. Monitoring indoor people presence in buildings using low-cost infrared sensor array in doorways. *Sensors*. 2021;21(12).

[9] Rey Gozalo G, Barrigón Morillas JM, Trujillo Carmona J, Montes González D, Atanasio Moraga P, Gómez Escobar V, et al. Study on the relation between urban planning and noise level. *Applied Acoustics*. 2016;111:143-7.

[10] Rey Gozalo G, Gómez Escobar V, Barrigón Morillas JM, Montes González D, Atanasio Moraga P. Statistical attribution of errors in urban noise modeling. *Applied Acoustics*. 2019;153:20-9.

[11] Vidaña-Vila E, Duboc L, Alsina-Pagès RM, Polls F, Vargas H. BCNDataset: Description and analysis of an annotated night urban leisure sound dataset. *Sustainability* (Switzerland). 2020;12(19).

[12] Prabha S, Raghav RS, Moulya C, Preethi KG, Sankaran KS. Analysis and Monitoring Air Quality System using Raspberry PI. In: Proceedings of the 2020 *IEEE International Conference on Communication and Signal Processing, ICCSP 2020*. 2020. p. 1385-9.

[13] Arce P, Salvo D, Piñero G, Gonzalez A. FIWARE based low-cost wireless acoustic sensor network for monitoring and classification of urban soundscape. *Computer Networks*, 2021;196.

[14] Lopez-Ballester J, Pastor-Aparicio A, Felici-Castell S, Segura-Garcia J, Cobos M. Enabling Real-Time Computation of Psycho-Acoustic Parameters in Acoustic Sensors Using Convolutional Neural Networks. *IEEE Sensors Journal*. 2020;20(19):11429-38.

[15] UNE-EN 61672-1:2014. Electroacoustics- *Sound level meters- Part 1: Specifications*. Spanish Association for Standardization and Certification (AENOR)

[16] Gantuz, Miguel-Ángel, Peacock, Ignacio. Real-time graphing sound level meter. Engineering School. Mendoza University. www.um.edu.ar/ojs-new/index.php/FAI/article/download/798/787.

[17] IRAM 4074. *Sound Level Meter. General Specifications*. Argentine Institute of Standardization and Certification. IRAM. 1988;5.

[18] Horowithz, P, Hill W. *The Art of Electronics*, Cambridge University Press, Cambridge (United Kingdom), 2nd Edition, 1990.

[19] ISO 1996-1:2016. *Acoustics. Description, measurement and assessment of environmental noise. Part 1: Basic quantities and assessment procedures*. International Organization for Standardization: Geneva, Switzerland, 2016.

[20] ISO 1996-2:2017. *Acoustics — Description, measurement and assessment of environmental noise — Part 2: Determination of sound pressure levels*. International Organization for Standardization: Geneva, Switzerland, 2017.